

Analysis of x-ray linear dichroism spectra for NiO thin films grown on vicinal Ag(001)Y. Z. Wu,^{1,2,*} Y. Zhao,³ E. Arenholz,⁴ A. T. Young,⁴ B. Sinkovic,³ C. Won,⁵ and Z. Q. Qiu²¹*Department of Physics, Applied Surface Physics State Key Laboratory, and Advanced Materials Laboratory, Fudan University, Shanghai 200433, People's Republic of China*²*Department of Physics, University of California at Berkeley, Berkeley, California 94720, USA*³*Department of Physics, University of Connecticut, Storrs, Connecticut 06269, USA*⁴*Advanced Light Source, Lawrence Berkeley National Laboratory, Berkeley, California 94720, USA*⁵*Department of Physics, Kyung Hee University, Seoul 130-701, Korea*

(Received 10 May 2008; published 15 August 2008)

Antiferromagnetic (AFM) NiO thin films are grown epitaxially on vicinal Ag(118) substrate and investigated by x-ray linear dichroism (XLD). We find that the NiO AFM spins exhibit an in-plane spin-reorientation transition from parallel to perpendicular to the step edge direction with increasing the NiO film thickness. In addition to the conventional L_2 absorption edge, XLD effect at the Ni L_3 absorption edge is also measured and analyzed. The results identify a small energy shift of the L_3 peak. Temperature-dependent measurement confirms that the observed XLD effect in this system at the normal incidence of the x rays originates entirely from the NiO magnetic ordering.

DOI: [10.1103/PhysRevB.78.064413](https://doi.org/10.1103/PhysRevB.78.064413)

PACS number(s): 75.25.+z, 75.50.Ee, 75.70.Ak, 78.70.Dm

I. INTRODUCTION

Antiferromagnetic (AFM) thin films have been applied to many spintronics devices because of their characteristic magnetic properties, especially because of the so-called exchange bias effect, which induces a unidirectional magnetic anisotropy in field-cooled antiferromagnet-ferromagnet (AFM-FM) systems.¹ Although a complete understanding of the exchange bias effect has not been achieved yet, it is believed that the spin structure of the AFM materials plays an important role.^{2–4} Compared to the research on ferromagnetic (FM) materials, it remains an experimental challenge to probe the spin structure of AFM thin films because of its zero net spin. In recent years, soft x-ray magnetic linear dichroism (XMLD) in x-ray absorption (XA) has been developed into a powerful tool to study AFM materials.^{5,6} XMLD measures the difference in absorption coefficient across a core threshold for different angles of linear polarization relative to the sample crystallographic axes.^{5–8} In addition, XMLD also provides magnetic contrast with chemical and surface sensitivities.^{9–12} By measuring the XMLD effect, e.g., at the transition-metal $L_{3,2}$ absorption edges, the local spin direction of the AFM materials can be determined and under certain conditions the AFM magnetic domains can also be imaged using photoemission electron microscopy.^{9–12} Together with the x-ray magnetic circular dichroism effect, which determines the FM spin structure, the XMLD effect in NiO films has become a powerful tool for the study of the magnetic exchange interaction in AFM-FM systems.^{10–12} For example, a spin reorientation of NiO interfacial spins¹⁰ and a creation of a planar AFM domain wall¹³ have been observed in NiO/Co system. Zhu *et al.*¹⁴ also showed that the onset of the exchange bias in NiO/Co₈₄Fe₁₆ bilayers is accompanied by a preferential repopulation of the NiO AFM domains—a key component to the exchange bias.

The correct interpretation of XMLD data is not trivial and relies on the detailed understanding of polarization dependent effects in soft XA of magnetic and nonmagnetic origins.

Until very recently, the NiO spin axis was assigned by assuming that the higher-energy peak of the Ni L_2 doublet in an XA spectrum reaches its maximum value when the x-ray polarization vector \mathbf{E} is parallel to the Ni²⁺ spin axis.⁷ However, this interpretation was recently revised by Arenholz *et al.*,¹⁵ who showed that this assumption is correct only for the Ni spins parallel to the [100] crystalline direction and that the XMLD effect exhibits a strong anisotropy, i.e., angular dependence. In addition to the complexity of the magnetic contribution to the x-ray linear dichroism (XLD) effect, the crystal electric field also affects the XA spectra. For example, Haverkort *et al.*¹⁶ reported that there exists a strong XLD effect even for 1 ML NiO on Ag(001) at room temperature, which is above its Néel temperature, and that simultaneously the Ni L_3 absorption peak exhibits a 0.35 eV energy shift for the spectra with the polarization parallel and perpendicular to the film plane. In general, the existence of the crystal-field effect makes it difficult to isolate the magnetic contribution from the overall XLD effect. Therefore, an interesting question is whether it is possible to tailor a system in which the crystal-field effect is eliminated and the linear dichroism is of purely magnetic origin. In our previous report, we already demonstrated that the atomic steps can induce the AFM anisotropy for the NiO film grown at room temperature on vicinal Ag(001) surface.¹⁷ In this paper, we report a study of XLD in NiO films grown on vicinal Ag(001) with the steps parallel to the [110] direction at higher-growth temperature. We first confirmed that the XLD effect at the L_2 edge in this system is of purely magnetic origin at the normal incidence of x rays. Then we show that the atomic steps induce an in-plane uniaxial magnetic anisotropy with an in-plane spin-reorientation transition from parallel to perpendicular directions with respect to the step edges as the NiO thickness increases above the 3.5 nm. The XLD spectrum near the Ni L_3 edge was also carefully measured and analyzed and a purely magnetic order induced L_3 -edge XLD has been clarified in this system at the normal-incidence geometry.

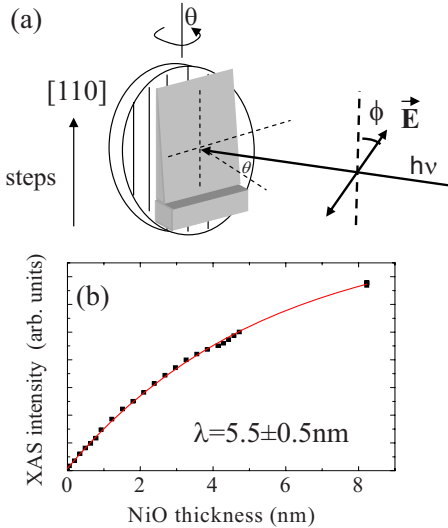


FIG. 1. (Color online) (a) Schematic drawing of the experimental geometry. (b) XAS intensity of the Ni L_3 peak at normal incidence of the x ray as a function of the NiO thickness. The solid line represents the fitting result (see text).

II. EXPERIMENT

A 10-mm-diameter Ag(118) single crystal (10° vicinal angle with steps parallel to [110] direction) was used as the substrate. The substrate was mechanically polished down to a $0.25 \mu\text{m}$ diamond-paste finish, followed by a chemical polishing,¹⁸ and then further cleaned in an ultrahigh vacuum (UHV) system by cycles of Ar^+ sputtering at $\sim 1.0 \text{ keV}$ and annealing at 600°C . NiO films were prepared by evaporating Ni in oxygen at a pressure of $\sim 1 \times 10^{-6}$ Torr onto the Ag substrate kept at 200°C . The film quality is further improved by post-growth annealing the film at 300°C under UHV conditions. The NiO thickness is determined by the Ni-deposition rate ($\sim 0.5\text{--}1.0 \text{ \AA}/\text{min}$) monitored by a quartz thickness monitor. It was shown earlier that under these conditions, NiO forms high-quality single-crystal film on Ag(001).^{19,20} In order to systematically study the thickness-dependent XLD effect, the NiO film was grown into a wedge shape by moving the substrate behind a mask. The wedge's slope is $\sim 1 \text{ nm}/\text{mm}$ with the layer thickness increasing along the atomic-step direction. Much thicker NiO film was grown at the end of the wedge for the purpose of clearly marking the NiO wedge position on the substrate.

The x-ray absorption spectroscopic (XAS) measurements were carried out at beamline 4.0.2 of the Advanced Light Source at the Lawrence Berkeley National Laboratory,²¹ which provides x ray with $99 \pm 1\%$ linear polarization. The XAS spectra were measured at different angles of incidence (θ) and polarization orientation (ϕ) as shown in Fig. 1(a), where the angle of incidence (θ) is defined as the angle between the x-ray beam and the sample surface-normal direction while ϕ is defined as the angle between the E vector of the incoming x-ray beam and the atomic-step direction of the Ag substrate. It should be noted that the ϕ dependence of XAS was studied by rotating the photon polarization direction while keeping the sample orientation fixed, which was

made possible by the elliptically polarized undulator at beamline 4.0.2. The XA spectra of the $\text{Ni}^{2+} L_{2,3}$ edges were recorded at room temperature in total electron yield (TEY) mode by monitoring the sample current. The high-temperature spectra were collected by measuring the electron yield using an electron channeltron. The linear background has been subtracted for all the XAS spectra shown in this paper. The thickness-dependent measurements were obtained by laterally moving the sample along the wedge direction with a precision of $< 0.1 \text{ mm}$. The x-ray beam size in the wedge direction is determined by the x-ray entrance slit width ($20 \mu\text{m}$).

III. RESULT AND DISCUSSION

Figure 1(b) shows the thickness dependence of the $\text{Ni}^{2+} L_3$ -edge absorption edge in normal incidence ($\theta=0^\circ$). It clearly shows that the intensity increases monotonically with the NiO thickness in the form of $I_{\text{NiO}} = I_{\text{NiO}}^\infty [1 - \exp(-d_{\text{NiO}}/\lambda_{\text{NiO}})]$, where the I_{NiO}^∞ is the NiO absorption intensity for infinite NiO thickness and λ_{NiO} is a phenomenological parameter that reflects the overall effect of the secondary-electron escaping distance and the x-ray penetration depth. The fitted value of $\lambda_{\text{NiO}} = 5.5 \pm 0.5 \text{ nm}$ is much greater than the secondary-electron escape depth of transition metals (Fe, Co, Ni) (Refs. 22 and 23) and noble metals (Au, Ag) (Ref. 24) but comparable with the value of rare-earth materials.²⁵ Since the x-ray penetration depth is larger than 20 nm ,²³ the fitted value λ_{NiO} should mainly reflect the secondary-electron escaping distance. The XAS in TEY mode measures all the electron escaping from the sample with energy higher than the work function and the low-energy secondary electron dominates the signal. In solids, inelastic lifetimes of excited electrons with energies larger than 1 eV above the Fermi level can be mainly attributed to the electron-electron (e-e) inelastic scattering with other processes such as electron-phonon and electron-imperfection interactions playing a minor role.^{24,26} Therefore, it is not surprising to observe a larger inelastic mean-free path in insulators in which the presence of an energy-band gap at the Fermi level reduces the inelastic e-e scattering channels.²⁷ To have a quantitative understanding of the inelastic lifetime of the low-energy electrons, the interplay between band structure and many-body effects on electron relaxation processes should be taken into account carefully,²⁸ which is out of the scope of this paper.

By measuring the Ni L_2 -edge XAS at different x-ray incident angles (θ), we confirmed that the NiO spins are oriented in the plane direction of the film in agreement with previous studies.^{7,9} To determine the spin direction within the film plane, we analyzed the ϕ dependence of the XAS at the normal incidence ($\theta=0^\circ$) [Fig. 1(a)]. XA spectra for $\vec{E} \parallel$ steps ($\phi=0^\circ$) and $\vec{E} \perp$ steps ($\phi=90^\circ$) were measured and the result clearly identifies the existence of the XLD effect [Fig. 2(a)]. As mentioned in Sec. I, the XLD effect is generally contributed from both the AFM ordering and the crystal-field effect. While the AFM contribution vanishes above the Néel temperature, the crystal-field contribution persists above the Néel temperature.¹⁶ The XAS result from our sample at the

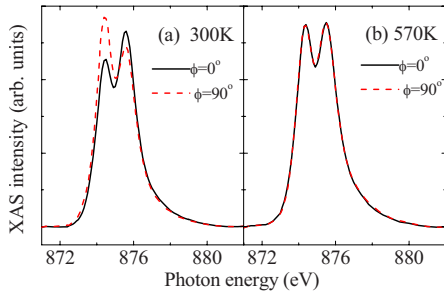


FIG. 2. (Color online) Ni L_2 -edge XAS of 4.3 nm NiO film measured at (a) room temperature and (b) 570 K at $\theta=0^\circ$.

normal incidence of the x rays shows an absence of the XLD effect at high temperature [Fig. 2(b)], indicating that the Ni L_2 -edge XLD in our system is solely of magnetic origin at the normal incidence of the x rays.

Figures 3(a)–3(c) show the representative pairs of XAS for the Ni L_2 edge for different NiO thicknesses. The Ni L_2 XA spectrum of a NiO film consists of two absorption peaks and the relative height of these two peaks is typically assumed to be determined by the angle between the x-ray polarization vector \vec{E} and the Ni spin orientation.^{7,13} The intensity difference of the XAS spectra between $\phi=0^\circ$ and 90° in Figs. 3(a)–3(c) clearly exhibits opposite behaviors below and above 3.5 nm NiO. For the 2.6 nm NiO film, the higher-energy peak for $\vec{E}\parallel\text{steps}$ ($\phi=0^\circ$) is less intense than that for $\vec{E}\perp\text{steps}$ ($\phi=90^\circ$) and the lower-energy peak for $\vec{E}\parallel\text{steps}$ ($\phi=0^\circ$) is greater than that for $\vec{E}\perp\text{steps}$ ($\phi=90^\circ$). Such behavior of the relative intensity of the Ni L_2 doublet is clearly reversed for the 4.7 nm NiO film. This fact indicates that the

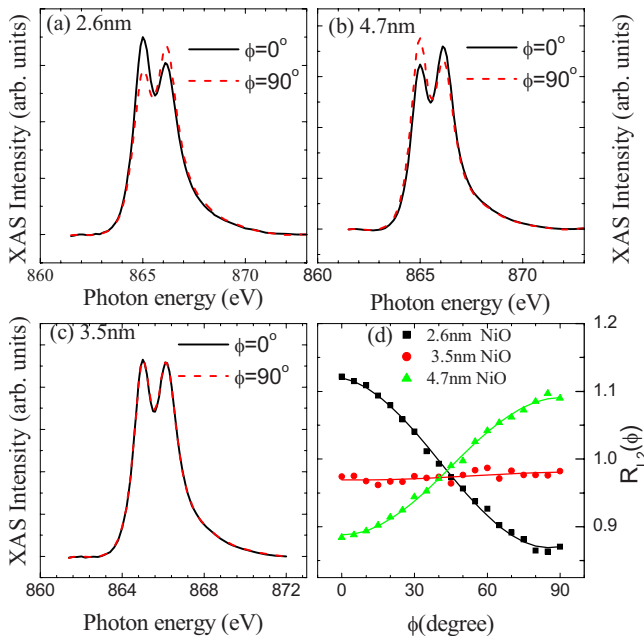


FIG. 3. (Color online) Ni L_2 -edge XAS of NiO films grown on Ag(118) at normal incidence of the x rays ($\theta=0^\circ$) at NiO thickness of (a) 2.6, (b) 4.7, and (c) 3.5 nm. (d) Ni L_2 ratio as a function of polarization angle ϕ for the NiO films in (a)–(c) and the solid lines in (d) are fitted results according to Eq. (1) as described in the text.

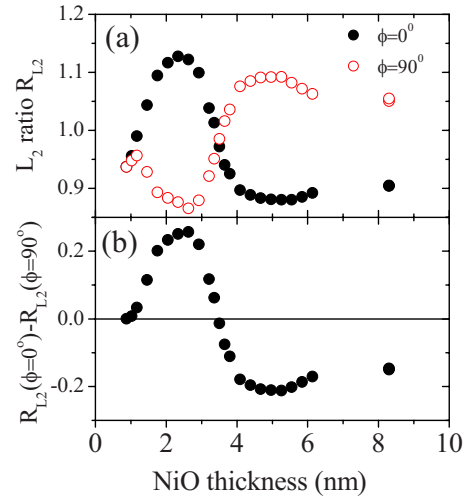


FIG. 4. (Color online) (a) Thickness-dependent L_2 ratio at the normal incidence of the x rays ($\theta=0^\circ$) or the x-ray polarization parallel ($\phi=0^\circ$) and perpendicular ($\phi=90^\circ$) to the atomic steps. (b) L_2 -ratio difference between $\phi=0^\circ$ and 90° as a function of the NiO thickness.

Ni²⁺ spin direction undergoes a directional switch with increasing the NiO thickness above the critical thickness of 3.5 nm, for which the NiO film does not show a difference in the XAS spectra between two photon polarization orientations [$\vec{E}\parallel\text{steps}$ ($\phi=0^\circ$) vs $\vec{E}\perp\text{steps}$ ($\phi=90^\circ$)]. It has been shown that the L_2 ratio (R_{L2}) of the XA spectrum, which is defined as the intensity ratio of the two Ni L_2 peaks (the lower-energy peak divided by the higher-energy peak), is related to the angle (β) between the x-ray polarization vector and the Ni²⁺-spin easy axis through simplified relation: $R_{L2}=A+B(3\cos^2\beta-1)$, with B being dependent on $\langle M^2 \rangle$ and A as representative of short-range nonmagnetic order.^{7,13} Then if ϕ_0 is the angle between the NiO spin axis and the step edge, the L_2 ratio at the normal incidence of the x rays should be described as

$$R_{L2} = A + B[3 \cos^2(\phi - \phi_0) - 1]. \quad (1)$$

Figure 3(d) shows the experimental values of the L_2 ratio as a function of ϕ for the three NiO thicknesses in Figs. 3(a)–3(c). The L_2 ratios of the NiO films show a clear sinusoidal ϕ dependence, which proves the validity of Eq. (1). As the thickness increases from 2.6 to 4.7 nm, we observe a change in the sign of the L_2 ratio with the extrema remaining at $\phi=0^\circ$ and 90° , showing that the Ni²⁺ spins undergo a 90° easy axis switching at ~ 3.5 nm NiO thickness.

More detailed thickness dependence of the XLD effect is shown in Fig. 4. For NiO thickness less than 1 nm, the L_2 ratio is independent of the x-ray polarization angle ϕ , showing an absence of the XLD effect. This is expected because the Néel temperature of the NiO film thinner than 1 nm is below the room temperature at which the experiment was performed. For NiO film thicker than 1 nm, the L_2 ratio exhibits a difference between $\phi=0^\circ$ and 90° , which is consistent with the establishment of an AFM order in the NiO film. The XLD value, which is defined as the L_2 ratio difference between $\phi=0^\circ$ and 90° , increases initially with the NiO

thickness with the L_2 ratio at \vec{E}_{\parallel} steps ($\phi=0^\circ$) greater than at \vec{E}_{\perp} steps ($\phi=90^\circ$), then switches the sign at ~ 3.5 nm NiO thickness, and reaches its negative maximum above 4 nm NiO thickness. It is worth to note that the above behavior for NiO films grown at 200 °C is different from a previous report on NiO films grown at room temperature,¹⁷ which may be due to a different structural relaxation of the NiO films at different growth temperature.²⁹ Whether a different growth temperature results in a different structural relaxation which in turn accounts for the observed difference in the NiO spin structures of the two samples requires further investigation and it is not the topic of this paper.

In previous studies of the Ni^{2+} XLD effect, it was assumed that for a magnetic generated XLD effect, the higher-energy peak of the L_2 doublet reaches its *maximum* value (or a *minimum* L_2 ratio) when the x-ray polarization vector is parallel to the Ni^{2+} spin direction. Recently, Arenholz *et al.*¹⁵ showed that the XMLD effect depends not only on relative orientation of the photon polarization and the spin axis but also on the crystallographic orientation. Although a detailed analysis of the XLD spectrum requires a complete ϕ -dependent measurement, one important consequence of Ref. 15 is that for the case of NiO, the XMLD (L_2 ratio) behaves in an opposite way for Ni spins along the [110] crystal axis as compared to Ni spins along the [100] axis, i.e., for Ni^{2+} spins parallel to [110] axis the higher-energy peak of the L_2 doublet should reach its minimum value (or a maximum L_2 ratio) when the x-ray polarization vector is parallel to the Ni spin direction. Assuming that the above result is held in our system, we can make a clear assignment of the Ni^{2+} spin axis based on the result of Fig. 3. First, since the Ni L_2 ratio reaches its extremum as the x-ray polarization vector is parallel to the atomic steps ([110] axis), we can conclude that the Ni spin direction is either parallel or perpendicular to the step [110] direction. Second, since the Ni spin-easy axis is parallel to the [110] crystal axis, we need to apply the Arenholz's result¹⁵ that the higher-energy peak of the L_2 doublet should reach its minimum value (or a maximum L_2 ratio) when the x-ray polarization vector is parallel to the Ni^{2+} spin direction. Therefore, we conclude from the result of Fig. 3 and Arenholz's work¹⁵ that the Ni^{2+} spins in our NiO/Ag(118) system is parallel to the steps below 3.5 nm NiO and perpendicular to the steps above 3.5 nm NiO.

Next we shift our attention to discuss the XMLD effect at the Ni L_3 edge in our NiO/Ag(118) system. As mentioned in Sec. I, NiO XLD effect should generally consist of both the magnetic and the crystal-field effects.¹⁶ The result of Fig. 2 shows that the XLD effect at the Ni L_2 edge for NiO films grown on vicinal Ag surface with the steps parallel to [110] comes *only* from the magnetic origin at the normal incidence of the x rays because the XLD effect vanishes above the NiO Néel temperature. Therefore, the NiO/Ag(118) system can be used to examine the magnetic- and crystal-field contributions to the XLD effect at the Ni L_3 edge separately. Figures 5(a) and 5(b) show the Ni L_3 -edge XAS measured on NiO films of 2 (Ni^{2+} spin parallel to the steps) and 6 nm (Ni^{2+} spin perpendicular to the steps) thicknesses, respectively. We first measured the XAS spectra at a 60° incident angle for two polarization directions and observed a strong XLD effect, in

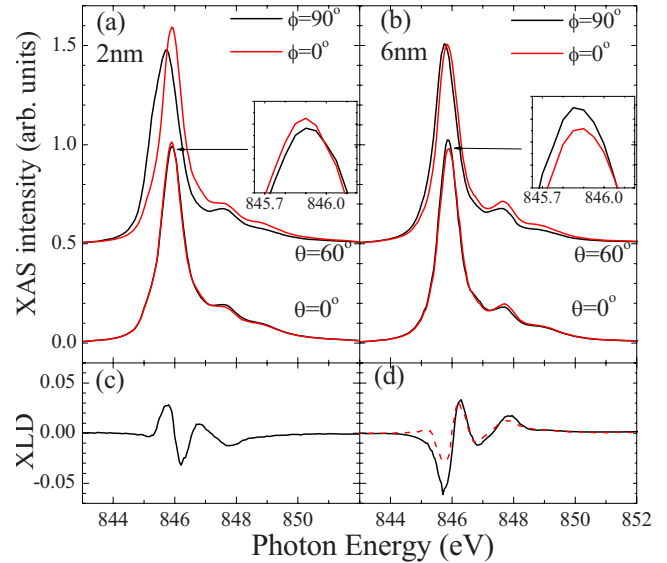


FIG. 5. (Color online) L_3 -edge NiO XAS spectra at different incident angles and polarization directions for NiO grown on Ag(118) with the thickness of (a) 2 and (b) 6 nm. The insets are the zoom-in L_3 peak at the normal incidence of the x rays. (c) and (d) are the XLD spectra of 2- and 6-nm-thick NiO films at the normal incidence of the x rays. The dashed line of XLD spectrum in (d) is the spectrum of (c) after reversing its sign.

particular for the 2 nm NiO film. Although the XAS line shape depends on many factors, the XAS peak shift is generally used as a signature of the crystal-field effect.¹⁶ Thus, we follow the same analysis in order to be consistent with the literature. Then it is obvious that the L_3 peak exhibits an energy shift toward higher energy for ϕ changes from 90° to 0° . Although the amount of this energy shift (ΔE) decreases with the NiO thickness ($\Delta E \sim 200$ meV for 2 nm NiO film and $\Delta E \sim 80$ meV for 6 nm NiO film), the L_3 peak shifts its energy in the same direction for both 2 and 6 nm NiO films. Noticing that the NiO film undergoes a spin-reorientation transition at 3.5 nm, the fact that the L_3 peak shifts its energy in the same direction for both 2 and 6 nm NiO films indicates that the L_3 -edge XLD effect in the NiO/Ag(118) at 60° x-ray incident angle is mainly contributed from the crystal-field effect, which is in agreement with a previous report.¹⁶ Then it is interesting to examine the L_3 -edge XLD effect at the normal incidence of the x rays where the crystal-field effect is absent at the L_2 edge. At the normal photon incidence ($\theta=0^\circ$), the L_3 XAS shows a small but detectable XLD effect with a small adsorption intensity difference and a tiny energy shift of $\Delta E = 18 \pm 2$ meV (see the inset of Fig. 5). Since this tiny energy shift is comparable to the energy reproducibility of the beamline, to reduce the uncertainty of the energy peak positions at the two polarizations, the XAS spectra reported here were measured by alternating the polarization at each energy of the XAS measurement. In this way, the spectra with two polarizations have exact same energy at each energy step of the measurement so that the error of the energy shift between the two polarizations can be minimized. The NiO L_3 peak shows a lower energy at $\phi=0^\circ$ than at $\phi=90^\circ$ for 2 nm NiO [see inset of Fig. 5(a)] and a higher energy at $\phi=0^\circ$ than at $\phi=90^\circ$ for 6 nm NiO [see inset of Fig. 5(b)].

Such energy shift of Ni L_3 peak should not come from the experimental misalignment, which should result in an energy shift with the same sign for all the NiO film thicknesses since the XA spectra shown in Fig. 5 are from the same sample. Recalling that the NiO exhibits an in-plane spin-reorientation transition at ~ 3.5 nm thickness, the above result reflects the fact that at the normal x-ray incidence, the XLD is mainly contributed from the magnetic effect. Since the Ni^{2+} spins were determined to be parallel to the steps at 2 nm and perpendicular to the steps at 6 nm, we conclude that the NiO L_3 peak exhibits a higher adsorption intensity and a lower-energy peak position for the x-ray polarization parallel to the spin direction. Figures 5(c) and 5(d) show the detailed XLD spectra (the difference of the XA spectra at $\phi=0^\circ$ and at $\phi=90^\circ$) at the normal incidence of the x ray for the 2 and 6 nm NiO films. Indeed these two XLD spectra show a great similarity apart from their opposite signs [for comparison the spectrum of Fig. 5(c) is plotted with reverted sign in Fig. 5(d)], which indicates the Ni^{2+} spin-reorientation transition. The smaller amplitude of the 2-nm-film spectrum is consistent with the fact that the Néel temperature of the 2 nm NiO is closer to room temperature than the 6 nm film. It is also worth noting that the XLD spectra we obtained on NiO film is similar to the spectra reported for the NiFe_2O_4 and $\text{Co/NiO}(001)$ systems.¹⁵

To further confirm that the XLD effect of the NiO L_3 edge arises solely from the magnetic effect at the normal incidence of the x ray, we performed high-temperature measurement on our samples. As shown in Fig. 6(a), the XLD effect of the 4.3 nm NiO film observed at room temperature and at the normal incidence of the x ray disappears at 570 K, which is above the bulk NiO Néel temperature of 523 K. This observation fully proves that the XLD effect at the NiO L_3 edge at $\theta=0^\circ$ comes completely from the magnetic effect. In contrast, the similarity of the two XLD spectra taken at room temperature and at 570 K for the $\theta=60^\circ$ case suggests that the XLD effect in this case comes mainly from the crystal-field effect [see Fig. 6(b)].

IV. SUMMARY

We find that there exists an in-plane spin-reorientation transition in NiO films grown on Ag(118) surface at 200 °C. The Ni spin direction is parallel to the step direction for NiO

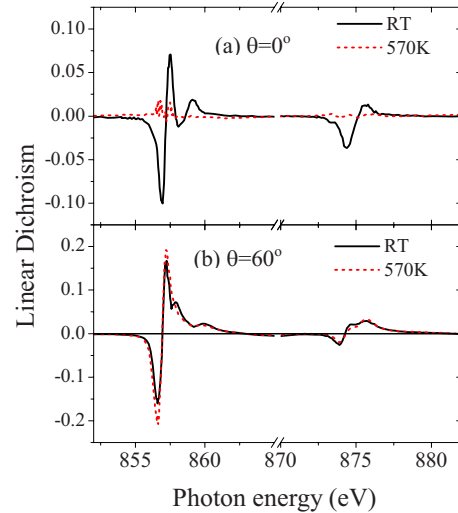


FIG. 6. (Color online) XLD spectra of 4.3 nm NiO film measured at room temperature and 570 K at different incident angles of the x ray: (a) $\theta=0^\circ$ and (b) 60° . The much smaller XLD signal and the absence of the XLD at 570 K at $\theta=0^\circ$ as compared to $\theta=60^\circ$ show that the XLD effect at $\theta=0^\circ$ comes mainly from the NiO AFM order while the XLD effect at $\theta=60^\circ$ is mainly contributed from the crystal-field effect.

films thinner than 3.5 nm and perpendicular to the steps for the films thicker than 3.5 nm. At the normal incidence of the x ray, we proved that the XLD effect at the Ni $L_{2,3}$ edges are solely of the magnetic origin and that the XA spectra at the L_3 edge exhibit a higher adsorption intensity and a tiny energy shift of $\Delta E=18 \pm 2$ meV toward the lower energy for x-ray polarization parallel to the spin direction than perpendicular to the spin direction.

ACKNOWLEDGMENTS

This work was supported by National Science Foundation under Grant No. DMR-0405259, by U.S. Department of Energy under Grant No. DE-AC03-76SF00098, by National Natural Science Foundation of China (973-project) under Grant No. 2006CB921303, by Shanghai Education Development Foundation, and by Fok Ying Tong education foundation.

*wuyizheng@fudan.edu.cn

¹W. H. Meiklejohn and C. P. Bean, Phys. Rev. **102**, 1413 (1956).
²J. Nogués and K. Ivan Schuller, J. Magn. Magn. Mater. **192**, 203 (1999).
³R. L. Stamps, J. Phys. D **33**, R247 (2000).
⁴M. Kiwi, J. Magn. Magn. Mater. **234**, 584 (2001).
⁵B. T. Thole, G. van der Laan, and G. A. Sawatzky, Phys. Rev. Lett. **55**, 2086 (1985).
⁶Pieter. Kuiper, Barry G. Searle, Petra Rudolf, L. H. Tjeng, and C. T. Chen, Phys. Rev. Lett. **70**, 1549 (1993).
⁷D. Alders, L. H. Tjeng, F. C. Voogt, T. Hibma, G. A. Sawatzky,

C. T. Chen, J. Vogel, M. Sacchi, and S. Iacobucci, Phys. Rev. B **57**, 11623 (1998).
⁸G. van der Laan, Phys. Rev. Lett. **82**, 640 (1999).
⁹J. Stöhr, A. Scholl, T. J. Regan, S. Anders, J. Lüning, M. R. Scheinfein, H. A. Padmore, and R. L. White, Phys. Rev. Lett. **83**, 1862 (1999).
¹⁰H. Ohldag, A. Scholl, F. Nolting, S. Anders, F. U. Hillebrecht, and J. Stöhr, Phys. Rev. Lett. **86**, 2878 (2001).
¹¹H. Ohldag, T. J. Regan, J. Stöhr, A. Scholl, F. Nolting, J. Lüning, C. Stamm, S. Anders, and R. L. White, Phys. Rev. Lett. **87**, 247201 (2001).

- ¹²F. Nolting, A. Scholl, J. Stöhr, J. W. Seo, J. Fompeyrine, H. Siegwart, J.-P. Locquet, S. Anders, J. Lüning, E. E. Fullerton, M. F. Toney, M. R. Scheinfein, and H. A. Padmore, *Nature (London)* **405**, 767 (2000).
- ¹³A. Scholl, M. Liberati, E. Arenholz, H. Ohldag, and J. Stöhr, *Phys. Rev. Lett.* **92**, 247201 (2004).
- ¹⁴W. Zhu, L. Seve, R. Sears, B. Sinkovic, and S. S. P. Parkin, *Phys. Rev. Lett.* **86**, 5389 (2001).
- ¹⁵Elke Arenholz, Gerrit van der Laan, Rajesh V. Chopdekar, and Yuri Suzuki, *Phys. Rev. Lett.* **98**, 197201 (2007).
- ¹⁶M. W. Haverkort, S. I. Csiszar, Z. Hu, S. Altieri, A. Tanaka, H. Hsieh, H.-J. Lin, C. T. Chen, T. Hibma, and L. H. Tjeng, *Phys. Rev. B* **69**, 020408(R) (2004).
- ¹⁷Y. Z. Wu, Z. Q. Qiu, Y. Zhao, A. T. Young, E. Arenholz, and B. Sinkovic, *Phys. Rev. B* **74**, 212402 (2006).
- ¹⁸N. Q. Lam, S. J. Rothman, and L. J. Nowicki, *J. Electrochem. Soc.* **119**, 715 (1972).
- ¹⁹C. Giovanardi, A. di Bona, and S. Valeri, *Phys. Rev. B* **69**, 075418 (2004).
- ²⁰C. Lamberti, E. Groppo, C. Prestipino, S. Casassa, A. M. Ferrari, C. Pisani, C. Giovanardi, P. Luches, S. Valeri, and F. Boscherini, *Phys. Rev. Lett.* **91**, 046101 (2003).
- ²¹A. T. Young, E. Arenholz, S. Marks, R. Schlueter, C. Steier, H. A. Padmore, A. Hitchcock, and D. G. Castner, *J. Synchrotron Radiat.* **9**, 270 (2002).
- ²²Y. Z. Wu, C. Won, A. Scholl, A. Doran, F. Toyoma, X. F. Jin, N. V. Smith, and Z. Q. Qiu, *Phys. Rev. B* **65**, 214417 (2002).
- ²³R. Nakajima, J. Stöhr, and Y. U. Idzerda, *Phys. Rev. B* **59**, 6421 (1999).
- ²⁴H. Kanter, *Phys. Rev. B* **1**, 522 (1970).
- ²⁵B. T. Thole, G. van der Laan, J. C. Fuggle, G. A. Sawatzky, R. C. Karnatak, and J. M. Esteve, *Phys. Rev. B* **32**, 5107 (1985).
- ²⁶P. M. Echenique, J. M. Pitarke, E. V. Chulkov, and A. Rubio, *Chem. Phys.* **251**, 1 (2000).
- ²⁷Koicho Kanaya, Susumu Ono, and Fumiko Ishigaki, *J. Phys. D* **11**, 2425 (1978).
- ²⁸I. Campillo, J. M. Pitarke, A. Rubio, E. Zarate, and P. M. Echenique, *Phys. Rev. Lett.* **83**, 2230 (1999).
- ²⁹C. Giovanardi, A. di Bona, S. Altieri, P. Luches, M. Liberati, F. Rossi, and S. Valeri, *Thin Solid Films* **428**, 195 (2003).